ERROR ANALYSIS OF FACSIMILE CAMERA MAPPING

Sherman S.C. Wu, Supervisory Physical Scientist

United States Geological Survey, Flagstaff, AZ 86001
USA
Commission V

ABSTRACT

Imagery from facsimile cameras is composed of image elements recorded by scanning in both horizontal and vertical directions. The solution to the problem of photogrammetric mapping using such close-range images, as from the Mars Viking Landers, is to convert the scanning imagery to the equivalent of a frame picture so that the presently available analytical plotters can be used for map compilation. The off-line conversion is carried out by digital image processing techniques whereas on-line conversion is performed in real time during the process of map compilation on the plotter. The mapped area is about 6 m by 8 m in front of the two cameras with a fixed base of 0.821 m between the two facsimile cameras. The map scale is 1:10 with a contour interval of 1 cm. Mapping precision depends on camera performance and image resolution, and varies over the mapped area. With appropriate geometric corrections made to high-resolution images (0.04°), horizontal precision varies from 0.008 m to 0.140 m at points from front center to far corners of the mapped area. Using low-resolution images (0.12°), map precision ranges from 0.023 m to 0.420 m.

INTRODUCTION

Two facsimile cameras (Tompkins, 1965) were installed on each of the two Viking Landers for close-up imaging of the Martian surface. The scene was converted to electrical signals by a photosensor array in the cameras according to variations in light intensity. Signals were then transmitted to Earth in digital form. Pictures reconstructed by ground reconstruction equipment are equivalent to imagery on a spherical surface due to the fact that image elements were obtained by rotating the camera in the azimuth direction and scanning with a mirror in the elevation direction. Two approaches, off-line and on-line, have been developed for the solution of photogrammetric compilation using images from facsimile cameras (Wu, 1979). Compilations of maps of the two Viking Lander areas are limited to ranges of from 2 m to 8 m (Wu and Schafer, 1982) due to the small base which is 0.821 m between the two cameras. This paper analyzes mapping precision using fixed-base facsimile cameras.

IMAGE FORMAT

The focal length of the facsimile cameras installed on the two Viking Lander vehicles is 2.1143 inches (53.703 mm) (Itek Corp., 1972, 1974). There are 12 silicon photodiodes in the photosensor array (PSA) in the camera (Fig. 1), four of which are unfiltered diodes with an angular resolution of 0.04° (high resolution), they are used for imaging objects at different distances from 1.9 m to 13.3 m; all the other eight multispectral photodiodes have an angular resolution of 0.12° (low resolution), they are placed for objects at distances from 1.7 m to infinity with an optimum focusing distance of 3.7 m. One of the eight low resolution diodes is a survey mode diode and the rest are for color and infrared images. Pixel spacings for azimuth and elevation are equal; therefore, each pixel can be

represented in a spherical coordinate system consisting of azimuth, elevation and a grey level value.

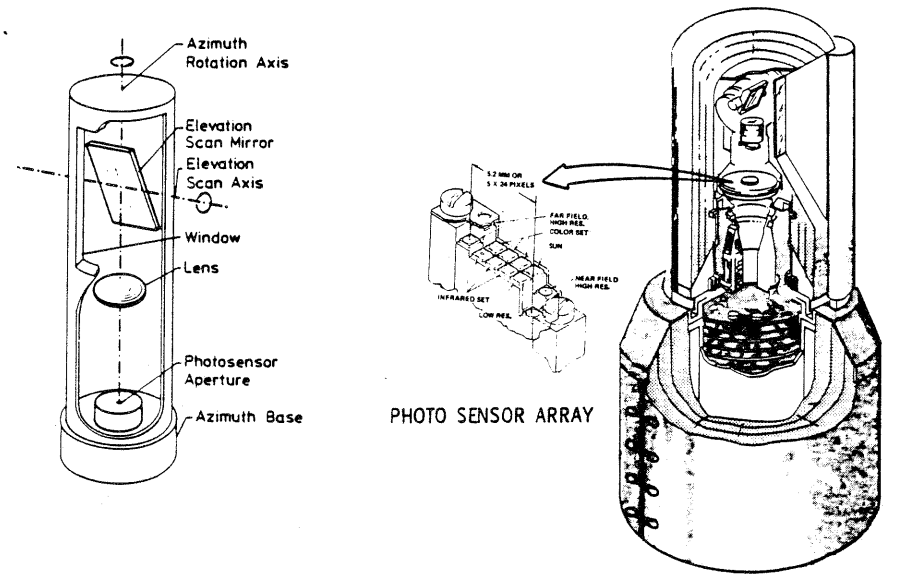

(a) (b)

Fig. 1(a) Basic optical components of the facsimile camera. (b) Facsimile camera and the photosensor array. The light ray from the ground object is reflected by a scanning mirror to a lens that focuses images of the incoming light through an aperture onto a photosensor, which then generates electrical signals that vary according to light intensity. The mirror is rotated in the vertical direction by a servo. For scanning in the azimuth direction, the camera rotates about the vertical axis in a stepwise fashion under servo control.

A total of 512 pixels is scanned in each vertical scan line covering 20.48° in high resolution modes and 61.44° in low resolution modes with depression angles varying in 10° increments. The picture width varies in 2.5° intervals up to 342.5°. The ground resolution of the camera ranges from 2 mm at the footpad of the spacecraft to 8 mm at a distance of about 5.5 mm (Mutch et al., 1972).

The photodiodes are off the optical axis by 0.48° in azimuth and the broadband diodes by 2.4° in elevation, therefore, the scan lines in object space lie on a cone (Wolf, 1975). This causes a systematic error in azimuth angles as a function of the elevation angle. The correct azimuth, Az_p, is obtained by:

$$Az_p = Az_c + \Delta Az \qquad (1)$$

$$\Delta Az = \text{Arc tan } \frac{\tan \alpha}{\cos E} - \alpha$$

Where Az_c is the recorded azimuth and ΔAz is the coning correction; E is the elevation angle of the point in question; $\alpha = \pm .48^0$, α is positive

for photodiodes BB2, BB4 and color modes at the left side, and negative for BB1, BB3 and survey modes at the right side of the camera axis. Coning correction is applied to the azimuth of the image point before rectification is made (Wu and Schafer, 1982).

SOLUTION OF THE MAPPING PROBLEM

Two approaches have been developed for the solution of the mapping problems using facsimile camera images. Using the off-line approach, images are converted to a format equivalent to central-point perspective frame pictures, enabling photogrammetric compilation in presently available analytical plotter software. The on-line approach is to modify the existing plotter software, thus, conversion and correction computations can be performed in real time during the compilation on the analytical plotters. Both methods use the same conversion equations (Richardus and Adler, 1972):

$$x = f \frac{\text{Sin } \Delta\lambda}{\text{Sin } E_o \tan E_p + \text{Cos } E_o \cos \Delta\lambda} \qquad (2a)$$

$$y = f \frac{\text{Cos } E_0 \tan E_p - \sin E_o \cos \Delta\lambda}{\sin E_o \tan E_p + \cos E_o \cos \Delta\lambda} \qquad (2b)$$

where $\Delta\lambda$ and E_p are azimuth and elevation elements of an image point; E_o is the elevation angle of the camera axis. The off-line approach was performed on a PDP 11/45 mini-computer using a program which performs linear interpolation of a 40 by 20 control grid using equations 2a and 2b. The linear interpolation produced errors as large as 15 mm on the ground. The on-line approach was tested on an AS-11AM analytical plotter which is interfaced with a Modcomp computer. This computer has a core memory of 64,000 words, Fortran programmable. Peripheral devices with the computer include 2 cartridge discs and 1 moveable-head disc (1.6 million bytes), 2 magnetic tape drives, 1 card reader, 1 line printer and one DEC terminal writer. After modification is made to the existing plotter software (operating system), this plotter is able to use unrectified raw pictures taken by facsimile cameras and perform map compilation and real-time corrections. This is, to date, the most accurate method of mapping the two Viking Lander areas on an analytical plotter. The error analysis made is based on the on-line approach using facsimile camera images on the AS11-AM analytical plotter.

ERROR ANALYSIS

As shown in Figure 1, the facsimile camera is an optical-mechanical type of scanner comprised of an optical system and an array of photosensors. The photogrammetric accuracy, aside from the effect of image resolution, is primarily determined by the performance of the servo mechanisms. Analysis by Huck et al. (1975) give maximum angular errors of ±0.15° and ±0.30° for azimuth and elevation respectively, in the low-resolution images; and ±0.1° and ±0.2° for azimuth and elevation respectively, in the high-resolution images. These figures include all errors of the servo mechanisms, position of the photosensor array and the camera mounting deviations. The errors amount to less than two pixels in low resolution photography, about three pixels in high-resolution photography along the azimuthal direction, and about twice these values in the elevation direction because of the mirror reflection. Therefore, these figures will determine the absolute map

precision, whereas the image resolution, the smallest resolvable image element, can be used to determine the relative precision, in the analysis of the mapping precision using images from facsimile cameras.

As shown in Figure 2(a) and (b), if X_c, Y_c, and Z_c, in the Viking Lander camera coordinate system (Von Struve, 1975), are coordinates of a ground object of which ΔA_{z1} and ΔA_{z2}, and E_1 and E_2, are azimuth and elevation elements on photographs from cameras 1 and 2 respectively, and the base between the two cameras is designated by b which has a calibrated distance of 0.821 m (Itek Corp. 1974);

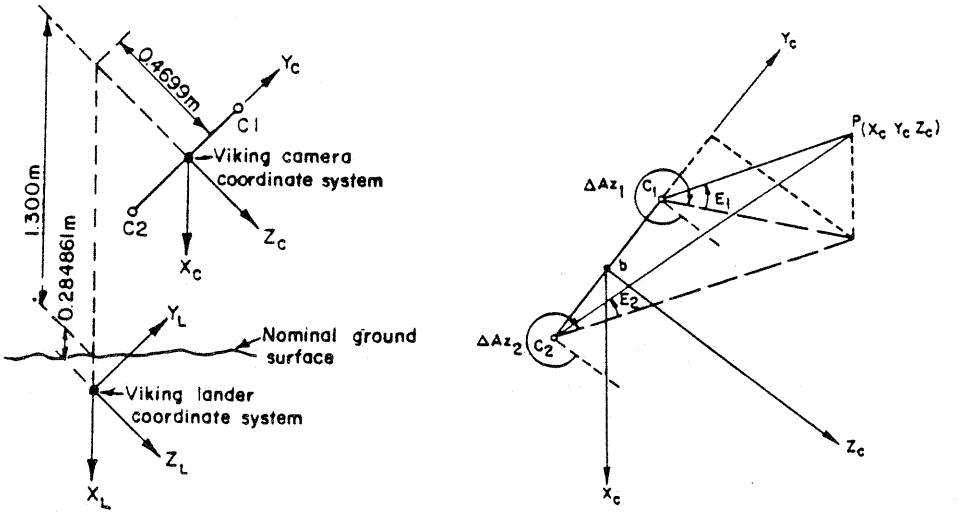

Fig. 2 Coordinate system: (a) Relationship of the cameras and the Lander coordinate system (LACS). C1 and C2 are the left and the right cameras, respectively, and the nominal base between C1 and C2 is 0.821 m. (b) Camera coordinate system.

$$Z_c = \frac{b}{\tan \Delta A_{z1} - \tan \Delta A_{z2}} \tag{3a}$$

$$Y_c = -\tfrac{1}{2} Z_c \, (\tan \Delta A_{z1} + \tan \Delta A_{z2}) \tag{3b}$$

$$X_C = -\tfrac{1}{2} Z_c \left(\frac{\tan E_1}{\cos \Delta A_{z1}} + \frac{\tan E_2}{\cos \Delta A_{z2}}\right) \tag{3c}$$

then, precison of these three coordinates can be determined by partially differentiating the equations with respect to their variable components. They can be expressed as:

$$\sigma_Z = \frac{Z^2}{b} \left(\sec^2 \Delta A_{z1} + \sec^2 \Delta A_{z2}\right) \sigma_{A_z} \tag{4a}$$

$$\sigma_y = \frac{Z}{b} \left[\left(Y + \frac{b}{2}\right) \sec^2 \Delta A_{z1} + \left(Y - \frac{b}{2}\right) \sec^2 \Delta A_z\right] \sigma_{A_z}$$

$$\text{for} \quad -\frac{b}{2} > Y > +\frac{b}{2} \tag{4b1}$$

$$\sigma_Y = \frac{Z}{b}\left[\left(Y - \frac{b}{2}\right)\sec^2 \Delta A_{z2} - \left(Y + \frac{b}{2}\right)\sec^2 \Delta A_{z1}\right]\sigma_{A_z}$$

$$\text{for} \quad -\frac{b}{2} \leq Y \leq +\frac{b}{2} \tag{4b2}$$

$$\sigma_X = -Z\left[\left\{\sec^2 \Delta A_{z1}\left(\frac{x}{b} - \frac{\sin \Delta A_{z1}}{2}\tan E_1\right)\right.\right.$$

$$\left. + \sec^2 \Delta A_{z2}\left(\frac{x}{b} - \frac{\sin \Delta A_{z2}}{2}\tan E_2\right)\right\}\sigma_{A_z}$$

$$\left. + \left\{\frac{\sec^2 E_1}{2\cos \Delta A_{z1}} + \frac{\sec^2 E_2}{2\cos \Delta A_{z2}}\right\}\sigma_E\right] \tag{4c}$$

$$\sigma_D = \frac{1}{D}(Z\,dZ + Y\,dY + X\,dX) \tag{5}$$

$$D = (Z^2 + Y^2 + X^2)^{1/2}$$

Using equations (4a) through (4c), relative and absolute mapping precisions using images of facsimile cameras on the two Viking Landers are calculated respectively with image resolution and uncertainties due to camera performance, i.e. for computing relative mapping precision, σ_{AZ} and σ_E are 0.04° and 0.12°, respectively for high- and low-resolution images; for computing absolute mapping precision, σ_{AZ} is 0.10° and 0.15°, and σ_E is 0.20° and 0.30°, respectively for high- and low resolution images.

Relative Precision - With the smallest resolvable image element (pixel) for both azimuth and elevation, as mentioned above, relative mapping precisions are calculated separately for each of the high- and low-resolution images as listed in Table 1. Precision of Z-coordinates, the ranges of objects, are calculated from 2 m to 6 m with increments of 1 m; precision of Y-coordinates, which are 90° to Z, and are left and right of the Z-axis, are calculated from -5 m to +5 m; and precision of X-coordinates, which are elevations of object points with positive toward the ground, are calculated from 0.0 m to -1.0 m with an increment of one-half meter. These figures cover the mappable areas of the two Viking Landers.

For example in Table 1, the map precision of Z, Y, and X from high resolution images are 9 mm, 4 mm, and 0 mm respectively for a point at the location of Z = 2 m, Y = 1 m, and X = -0.5 m. The precision of distance of the same point is 10 mm.

Absolute Precision - With angular uncertainties limited by the performance of the camera, also as mentioned above, absolute mapping precisions are calculated separately for each of the high- and low-resolution images as listed in Table 2. The actual mapping precision is considered better than the precision as listed in Table 2 due to the fact that the camera bolt

TABLE 1.- RELATIVE MAPPING PRECISION OF BOTH HIGH- AND LOW-RESOLUTION IMAGES FROM FACSIMILE CAMERAS OF THE TWO VIKING LANDERS

Resolution			High Resolution						Low Resolution					
Z(m)	Y(m)		0	±1	±2	±3	±4	±5	0	±1	±2	±3	±4	±5
		σ_z(mm)	7	9	14	22	34	50	21	26	42	67	103	149
		σ_y(mm)	1	4	13	33	67	123	4	12	40	98	202	368
		σ_D(MM)	8	10	20	40	76	132	23	30	59	119	227	396
2	x(m)													
	0.0		1	2	2	3	3	4	4	5	6	8	9	11
	-0.5	σ_x(mm)	0	0	1	3	5	9	1	1	4	9	16	26
	-1.0		2	2	5	8	14	21	5	7	14	25	41	62
		σ_z(mm)	16	17	22	31	43	58	47	52	67	93	128	174
		σ_y(mm)	2	6	15	30	56	96	6	17	44	91	169	288
		σ_D(mm)	17	20	28	45	72	114	51	59	85	135	217	342
3	x(m)													
	0.0		2	2	3	3	3	4	6	7	8	9	10	12
	-0.5	σ_x(mm)	0	1	1	2	4	6	1	2	3	6	11	17
	-1.0		3	3	5	7	11	15	8	10	14	21	32	45
		σ_z(mm)	27	29	34	43	55	70	82	88	103	128	164	210
		σ_y(mm)	3	7	17	32	54	87	8	21	51	95	162	260
		σ_D(mm)	30	32	41	56	80	115	89	97	122	168	239	344
4	x(m)													
	0.0		3	3	3	3	4	4	8	9	9	10	12	13
	-0.5	σ_x(mm)	1	1	1	2	3	4	2	2	3	5	8	13
	-1.0		4	4	5	7	10	13	11	13	16	21	29	39
		σ_z(mm)	43	45	50	56	70	85	128	134	149	174	210	256
		σ_y(mm)	4	9	20	35	56	85	11	26	59	104	167	254
		σ_D(mm)	46	49	57	71	93	124	138	146	170	213	279	373
5	x(m)													
	0.0		4	4	4	4	4	5	11	11	11	12	13	15
	-0.5	σ_x(mm)	1	1	1	2	2	4	2	2	3	5	7	11
	-1.0		5	5	6	7	9	12	15	15	18	22	28	36
		σ_z(mm)	62	63	68	77	89	104	185	190	205	230	266	312
		σ_y(mm)	4	10	23	38	59	86	13	31	68	114	176	259
		σ_D(mm)	66	68	76	90	111	140	197	204	228	270	333	420
6	x(m)													
	0.0		4	4	4	5	5	5	13	13	13	14	15	16
	-0.5	σ_x(mm)	1	1	1	2	2	3	3	3	4	5	7	9
	-1.0		6	6	7	8	10	12	18	18	20	24	29	35

REMARKS: σ_D is calculated for points with an x-value of -0.5 m.

TABLE 2 - ABSOLUTE MAPPING PRECISION OF BOTH HIGH- AND LOW-RESOLUTION IMAGES FROM FACSIMILE CAMERAS OF THE TWO VIKING LANDERS

	Resolution		High Resolution						Low Resolution					
Z(m)	Y(m)		0	±1	±2	±3	±4	±5	0	±1	±2	±3	±4	±5
		σ_z(mm)	18	22	35	56	86	124	27	33	52	84	129	186
		σ_y(mm)	4	10	33	86	169	306	5	15	50	123	253	460
		σ_D(mm)	20	26	50	100	190	331	29	39	74	150	285	496
2	x(m)													
	0.0		7	8	10	13	14	19	11	12	15	19	23	28
	-0.5	σ_x(mm)	3	3	2	1	5	12	5	4	3	1	8	19
	-1.0		0	1	6	14	26	42	0	2	9	21	39	63
		σ_z(mm)	39	43	56	77	107	145	58	65	84	116	161	218
		σ_y(mm)	5	14	36	76	141	240	8	21	55	114	211	360
		σ_D(mm)	43	50	71	113	182	286	65	75	107	169	273	429
3	x(m)													
	0.0		11	11	13	15	17	20	16	17	19	22	26	31
	-0.5	σ_x(mm)	4	4	4	2	0	4	7	6	6	3	0	5
	-1.0		1	2	5	10	17	27	2	3	7	15	26	41
		σ_z(mm)	69	73	86	107	137	175	103	109	129	161	205	263
		σ_y(mm)	7	18	42	79	135	217	11	27	63	119	203	326
		σ_D(mm)	75	82	102	140	200	287	113	123	154	211	300	431
4	x(m)													
	0.0		14	14	16	17	20	22	21	22	23	26	30	34
	-0.5	σ_x(mm)	6	6	5	4	3	1	9	8	8	7	4	1
	-1.0		2	3	5	8	14	21	3	4	7	13	20	31
		σ_z(mm)	107	111	124	145	175	213	161	167	186	218	263	320
		σ_y(mm)	9	22	49	86	139	212	13	33	74	129	208	318
		σ_D(mm)	116	122	142	178	234	311	173	183	214	268	350	467
5	x(m)													
	0.0		18	18	19	20	22	25	26	27	28	31	34	37
	-0.5	σ_x(mm)	7	7	7	6	5	4	11	10	10	9	8	5
	-1.0		3	4	5	8	12	17	5	5	8	12	18	26
		σ_z(mm)	154	158	171	192	222	260	231	237	256	288	333	390
		σ_y(mm)	11	26	56	95	147	216	16	39	85	143	220	323
		σ_D(mm)	165	171	191	226	278	351	247	257	286	339	417	526
6	x(m)													
	0.0		21	21	22	23	25	27	31	32	33	35	38	41
	-0.5	σ_x(mm)	8	8	8	8	7	6	13	12	12	11	10	9
	-1.0		4	4	6	8	11	15	6	7	9	12	17	23

REMARKS: σ_D is calculated for points with an x-value of -0.5 m.

down errors had been carefully calibrated and had been corrected in the mapping process (Wolf, 1976, Wu and Schafer, 1982).

Since one of the purposes of mapping the area surrounding the Viking Lander was to provide spatial information for guiding the sampler, for collecting soil for tests, precision of distances is also calculated using equation (5). This information was particularly important since the soil sampler was a rather sensitive device making samples in rocky areas hazardous.

REFERENCES

Huck, F. O., McCall, H. F., Patterson, W. R., and Taylor, G. R. 1975. The Viking Mars lander camera, Space Science Instrumentation 1, pp. 189-241.

Itek Corporation, 1972. Viking Lander imaging systems--image quality analysis report, Itek-2874-VLC-349, 97 p.

_____, 1974. Viking Lander imaging system--calibration report of lander camera system, Itek-5248-VLC-349, PD 6400432-029 and -039, 53 p.

Mutch, T. A., Binder, A. B., Huck, F. O., Levinthal, E. C., Morris, E. C., Sagan, Carl and Young, A. T., 1972. Imaging experiment--The Viking Lander, Icarus, v. 16, no. 1, pp. 92-110.

Richardus, Peter, and Adler, R. K., 1972. Map projections for geodesists, cartographers and geographers, Amsterdam, London, North-Holland, 174 p.

Tompkins, D. N., 1965. Lunar surface panoramic photography. Presented at the American Society of Photogrammetry, Sept. 23, 1965, Dayton, Ohio.

von Struve, H. C., 1975. Results of Lander Coordinate System meeting at Jet Propulsion Laboratory, October 9, 1975, Viking Flight Team Memorandum, reference LSG-13542-SLC, Oct. 17, 1975, 2 p.

Wolf, M. R., 1975. The analysis and removal of geometric distortion from Viking lander camera images. Presented at the 1975 fall convention, American Society of Photogrammetry and American Congress on Survey and Mapping, Oct. 26-31, 1975, Phoenix, Arizona.

_____, 1976. Jet Propulsion Laboratory memorandum to S. C. Wu., Reference 824-IPL/SIPG/76-192.

Wu, Sherman S. C., 1979. Topographic Mapping of Viking Lander Area, NASA Tech. Memorandum 80339: Report of Planetary Geology Program, 1978-1979, pp.425.

Wu, Sherman S. C. and Schafer, F. J., 1982. Photogrammetry of the Viking Lander Imagery, Photogrammetric Engineering and Remote Sensing, vol. 48, no. 5, pp. 803-816.